Influence of the dielectric constant anisotropy on the poling of ferroelectrics

K. Betzler[a]; B. Hellermann[a]; H. Hesse[a]

[a] Universität Osnabrück, Fachbereich Physik Postfach, Osnabrück

PLEASE SCROLL DOWN FOR ARTICLE

Influence of the Dielectric Constant Anisotropy on the Poling of Ferroelectrics †

K. BETZLER, B. HELLERMANN, AND H. HESSE

Universität Osnabrück, Fachbereich Physik
Postfach 4469, D 4500 Osnabrück

By calculating the potential distribution in ferroelectric crystals with applied electric field it is shown that — depending on the domain geometry — large field distortions occur which are due to the anisotropy of the dielectric susceptibility in ferroelectrics. These distortions can explain many of the problems showing up when poling crystals by an electric field.

For the application of ferroelectric materials it is often important to use single domain samples. Nearly all electro-, magneto-, and acousto-optical effects for instance depend on a directed polar axis throughout the crystal or at least its surface. Crystals exhibiting a Curie temperature near the growth temperature often can be poled during the growing process e. g. by applying an electric current [1]. For cases where this isn't possible, several methods have been developed to polarize crystals after growth [1,2]. The most evident and widest used is to treat the crystals in an electric field using the 'right mixture' of conditions as temperature, time, electrode material, applied field etc. In spite of all efforts in refining the recipes the result of the treatment is often unpredictable: 'Hard' domains do not switch, increasing the applied voltage leads to electric breakdown, and other effects occur.

In order to gain a more precise understanding of the physical effects in a crystal with applied poling voltage, we calculated the electric potential distribution inside a crystal for several simple geometries. The calculations show that the anisotropy of the dielectric susceptibility may be one reason for poling problems.

As material for our numerical considerations we chose $KNbO_3$ which exhibits two phase transitions from its melting point down to room temperature [3] and therefore cannot be poled during the growth process. The directions of spontaneous polarization in the orthorhombic room-temperature phase are parallel to the pseudocubic (110) directions, so several types of domain and domain-wall configurations are possible. For simplicity we took only two of these directions into account for our model geometries, namely (110) and ($\bar{1}$10). For these 90° domains, the walls show up at an angle of 45° to the polarization direction [4]. Furthermore we selected configurations where the crystal and field geometry varies in only two dimensions thus enabling us to neglect the third dimension in the calculation scheme. With these restrictions, the potential distribution in crystals with applied electric potential between parallel plate electrodes was calculated (for a detailed description of the mathematical treatment see the Appendix).

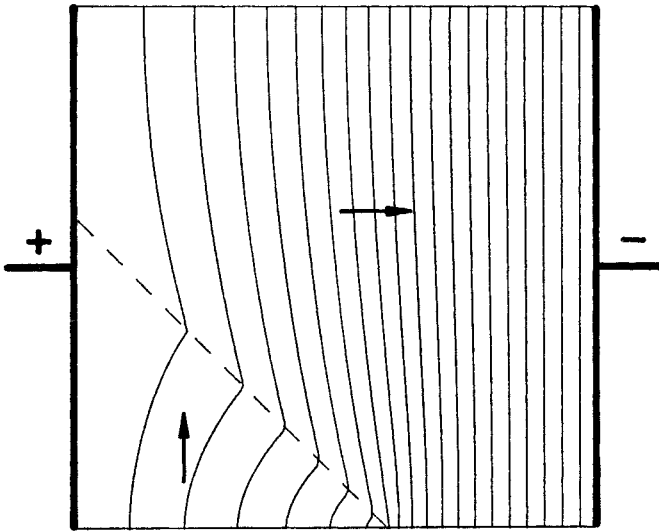†Communicated by Professor Horst Muser

Fig. 1: Potential contour plot of a crystal with a large poled and a small unpoled domain, the directions of the spontaneous polarizations are indicated by arrows.

Some of the results for simple geometries are shown in figs. 1–4 where the equipotential lines are drawn for the respective sample geometries (dashed lines indicate domain boundaries). The contour lines represent potential steps of 0.05 times the total applied potential $\varphi_{max} - \varphi_{min}$.

Fig. 1 shows the situation in a nearly single domain crystal with a small unpoled domain (here and furtheron 'poled'/'unpoled' is used for domains with their polar axis parallel/perpendicular to the applied electric field). The field in the poled region is considerably higher than in the unpoled, far away from the domain boundary the field should directly reflect the anisotropy of the dielectric susceptibility which is about one order of magnitude in $KNbO_3$. In a partially poled crystal the field in the unpoled region so may be lowered by up to one order of magnitude, a fact greatly hampering the poling process.

Another effect occuring at the boundary of 90° domains is better visible in fig. 2. Here a situation complementary to that of fig. 1 is depicted, a small poled region adjacent to a large unpoled region. The field in the unpoled region is not only smaller than in the poled one but — at least near the boundary — also points into a direction which will not force the polarization to switch into the desired direction. Such domain boundaries should be rather stable in spite of high applied voltages.

Fig. 3 shows the potential contour lines near the 90° corner of an unpoled domain in a poled region. The field in the poled region near the corner is enlarged similar to the situation near a metallic point. Electrical breakdown is rather probable in such configurations when the applied voltage is increased.

The potential distribution in a crystal with an inclusion of gas or other low dielectric medium (e. g. non ferroelectric material from the melt such as K_2O) is shown in
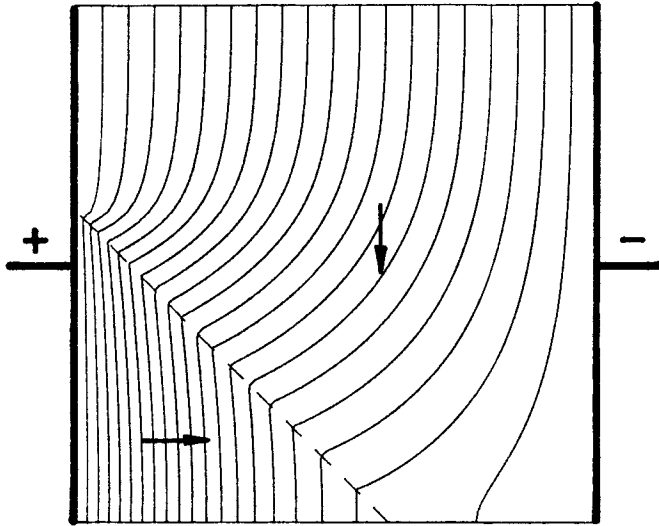
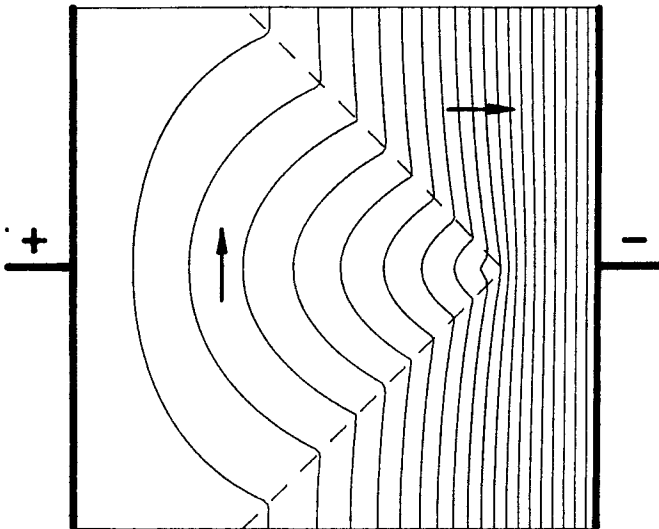Fig. 2: Complementary configuration to fig. 1.

Fig. 3: Potential distribution near a domain corner

fig. 4. The field distortion around the inclusion is rather dramatic and obviously will cause misoriented domains near the inclusion. Also the field in the included material is drastically increased thus leading to a greatly enhanced breakdown probability.

Conclusion. The calculations show that the anisotropy of the dielectric susceptibility leads to various effects during the poling of ferroelectric crystals by an electric field. Lowered fields in unpoled domains, 'wrong' field directions near domain boundaries and raised fields at domain edges causing breakdown often will make it impossible to obtain large single domain crystals only by applying an electric field. Other additional
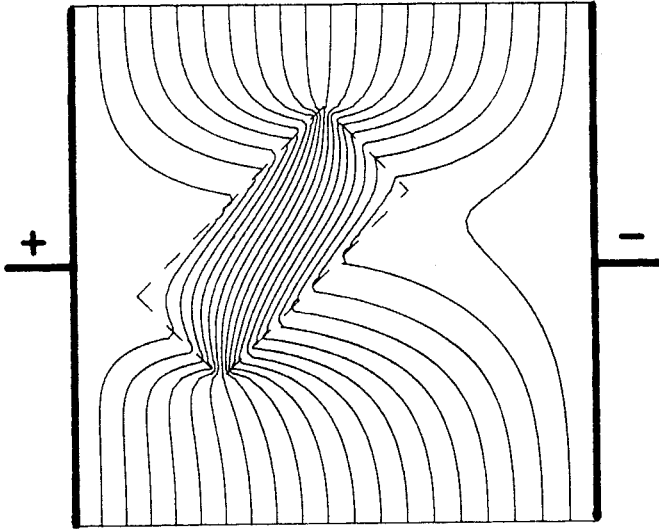
Fig. 4: Potential distribution at an inclusion of low dielectric material.

poling forces such as mechanical stress are necessary. Inclusions of gas or phases of low susceptibility greatly enhance these effects thus leading to a huge deformation of the surrounding electric field. New domains of undesired orientation will appear near these distortions.

Appendix. The potential distribution inside the model crystals was calculated by relaxation method on a two-dimensional regular rectangular mesh. Applying the Maxwell equations div $\vec{D} = 0$ and rot $\vec{E} = 0$ results in the iteration scheme for the electrostatic potential φ

$$\varphi_{n+1}(x,y) = f^{-1} \cdot \sum_{i=-1}^{1} \sum_{j=-1}^{1} \delta_{|i|+|j|,1} \cdot \epsilon\left(x + i\frac{a}{2}, \ y + j\frac{b}{2}\right) \cdot \varphi_n(x + ia, \ y + jb)$$

with the normalization factor

$$f = \sum_{i=-1}^{1} \sum_{j=-1}^{1} \delta_{|i|+|j|,1} \cdot \epsilon\left(x + i\frac{a}{2}, \ y + j\frac{b}{2}\right)$$

x, y: node coordinates and a, b: node spacing in x- and y-direction, respectively.

The susceptibility field ϵ is defined by the respective crystal geometry — at the side borders of the crystal symmetric border conditions are forced by appropriate settings of the ϵ-values. For starting the iteration the potential distribution in an 'empty' crystal is used. For each geometry the calculation was done on a 50 * 50 point mesh, the iteration was terminated when $\mathrm{Max}|\varphi_n(x,y) - \varphi_{n-1}(x,y)| < 10^{-6} \cdot |\varphi_{\max} - \varphi_{\min}|$. Considerable acceleration was achieved by starting on a 25 * 25 point submesh, then interpolating the potentials for the omitted points, and finally iterating on the 50 * 50

point mesh. The calculation then took about 40 minutes for one geometry on a personal computer with numeric coprocessor. From the calculated potential field contour lines were derived and plotted using standard contour plot routines.

To test the iteration program a well-known standard geometry was used — a low dielectric cylinder in a high dielectric medium [5]. The result for this test geometry is shown in fig. 5. The parallel equipotential lines reflect the homogeneous field inside the cylinder well known from theoretical physics lessons. The small deviations from the expected 'ideal' result are due to the interpolation scheme of the contour plot routines.
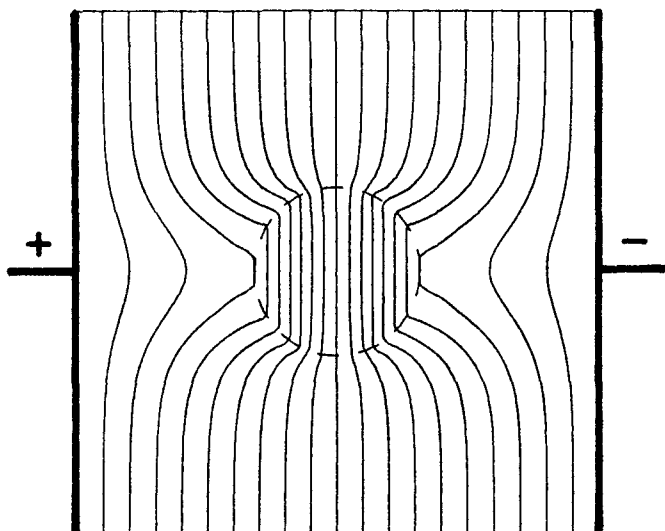

Fig.5: Contour plot of the potential distribution in the test geometry

REFERENCES

1. K. Nassau, H.J. Levinstein and G.M. Loiacono, J. Phys. Chem. Solids **27** (1966), 989–996.

2. T. Fukuda and Y. Uematsu, Japanese Journal of Applied Physics **11** (1972), 163–169.

3. E. Wiesendanger, Ferroelectrics **6** (1974), 263–281.

4. J. C. Burfoot, "Ferroelectrics", van Nostrand, London, 1967, pp. 200 ff.

5. L.D. Landau, E.M. Lifschitz, "Elektrodynamik der Kontinua", Akademie-Verlag, Berlin, pp. 51 ff.